AIAA JOURNAL
Vol. 37, No. 11, November 1999

Measurements of Supersonic Helium/Air Mixture Jets

Kevin W. Kinzie*
General Electric Aircraft Engines, Cincinnati, Ohio 45215
and
Dennis K. McLaughlin†
Pennsylvania State University, University Park, Pennsylvania 16802

An enhanced method of using helium/air mixture jets to simulate the aeroacoustic properties of hot jets is presented. By using helium to reduce the jet density and to increase the jet acoustic speed, unheated nominal Mach 1.5 jets are tested that have jet-to-ambient density and acoustic speed ratios that approximately match those from a hot jet with a jet-to-ambient static temperature ratio of 1.2. The jets are operated at a reduced Reynolds number (approximately 2.7×10^4), which allows the use of diagnostic measurement tools such as hot-wire anemometry and active control via glow discharge excitation. Mean and fluctuating flowfield and acoustic measurements from a near perfectly expanded Mach 1.5 elliptic and round jet are presented. Direct comparisons of the cold and simulated heated jets are made. Compared to the pure air jets, the helium/air mixture jets showed increased instability wave phase speeds near or exceeding the ambient acoustic speed, increased noise levels, and increased coupling between the flowfield fluctuations and the radiated acoustic field. These features are consistent with the theory of Mach wave radiation, the dominant noise source in high-speed jets. The data presented show that the helium/air simulation is able to capture the dominant noise characteristics of actual heated jets. The use of this group of diagnostic measurement techniques is an added benefit of the simulation that is not available in conventional heated jet experiments.

Nomenclature

A_t, A^*	= throat area
a	= speed of sound
D_{eq}	= area equivalent diameter
F	= Fliegner's constant
f	= frequency
f_c	= characteristic frequency, u_j/D_{eq}
M	= Mach number
$\dot{m}$	= mass flow rate
R	= distance from jet exit; gas constant
Sr	= Strouhal number, fD_{eq}/u_j
T	= temperature
u	= velocity
x	= axial distance from jet exit
γ	= ratio of specific heats
ρ	= density

Subscripts

a	= ambient property
c	= convective property
ch	= anechoic chamber property
j	= jet exit property
0	= stagnation quantity

Superscript

*	= simulated condition of helium/air mixture jet

Introduction

IN the field of jet noise research, many laboratory jet noise tests use unheated jets to represent flows from various nozzle configurations. However, a problem inherent to experiments with unheated jets is that, even at low supersonic Mach numbers, the large-scale turbulent structures may not achieve a supersonic phase speed. Morrison and McLaughlin[1] measured the phase speed of the dominant jet Strouhal number component to be only about three-quarters of the ambient sound speed for a cold Mach 1.5 circular jet. This would mean that the radiated noise would not contain Mach wave emission, a primary noise generator found in high-speed jets when the turbulent structure velocity exceeds the ambient sound speed. However, when a Mach 1.5 jet is heated, the jet velocity as well as the structure convection velocity increase significantly and can produce Mach wave radiation. In most practical applications, such as turbojet engine exhausts, the jet static temperature is well above the ambient temperature so the Mach wave emission may be present even in subsonic aircraft engines.

Research by Tanna et al.,[2] Lau,[3] Seiner et al.,[4] and Tam and Chen[5] demonstrates that there are significant differences in how moderately heated supersonic jets generate noise from their unheated counterparts. Therefore, to study jets under realistic engine operating conditions, they should be heated so that the convection velocity of the structures is supersonic and the effects of Mach wave radiation can be measured. In practical terms, however, a heated jet facility involves significant complexity and expense. To avoid this in the present work, the low density and high velocity of hot jets are simulated by using a lower density gas with different properties than air, namely, helium. This allows the jet properties to be compared as the operating conditions change from cold to simulated hot conditions so that the effects of jet heating can be directly observed. Although there are some differences between an actual heated jet and the simulation, the major features of the Mach wave emission process are well represented by the simulated jet. Therefore, the primary noise generation mechanism found in heated jets is also present in the helium simulation.

A research program at the Pennsylvania State University has been investigating supersonic jet noise generated from round and asymmetric jets. There are three unique aspects to this work. The first is that the experiments were performed under reduced Reynolds number conditions. This is an approach that has been applied successfully in the same facility when it was located at Oklahoma State University.[1,6,7] The approach involves operating jets at a Reynolds number much lower than that found in actual jet engines. Work from Refs. 1, 6, and 7 confirms that the low-to-moderate Reynolds number

Received 27 April 1998; presented as Paper 98-2328 at the AIAA/CEAS 4th Aeronautics Conference, Toulouse, France, 2–4 June 1998; revision received 16 April 1999; accepted for publication 14 May 1999.

*Lead Engineer, Installation Aero Technology; currently Aerospace Engineer, Aeroacoustics Branch, NASA Langley Research Center, MS 166, Hampton, VA 23681. Senior Member AIAA.

†Professor and Head, Department of Aerospace Engineering. Associate Fellow AIAA.

Table 1 Properties of Mach 1.5 jet for different gases and temperature conditions

Case	T_0, K	Jet He concentration (by mass), %	Ambient He concentration (by mass), %	U_j, m/s	a_j, m/s	a_a, m/s	ρ_a/ρ_j	Actual T_j/T_a	γ_j
A	293	0	0	430	290	343	0.69	0.69	1.4
B	293	26	0	690	460	343	1.5	0.61	1.55
C	293	26	7	690	460	415	1.2	0.61	1.55
D	760	0	0	690	460	343	1.8	1.8	1.4
E	760	0	0	690	460	415	1.2	1.2	1.4

supersonic axisymmetric jets produce noise that, when scaled properly, is very similar in level and directivity to jets operating at much higher Reynolds numbers. The second unique aspect of this work is that high-speed heated jets are simulated by mixing helium with the jet airflow. The helium/air mixture jets are designed to simulate the low density and high velocity of hot jets. Most of the data, analysis, and interpretation of the data have been presented previously.[8-11] The third unique aspect of this research is that the jets are sometimes excited with a glow discharge excitation, a form of active control.

The purpose of this paper is to document the development and methodology of the helium/air simulation and to demonstrate its usefulness in this research. The analysis required to properly produce a helium/air mixture and explain how it simulates an actual heated jet is presented. Jet aerodynamic and acoustic measurements are presented to show how these properties are affected when helium is used to simulate hot jet temperatures. Similarities and differences between the simulated hot jets and actual hot jets are discussed.

Heated Jet Simulation

As described in McLaughlin et al.,[9] the jet noise facility has been modified to mix helium with the main jet airflow. The jet then has a reduced density and higher acoustic speed (and jet velocity) compared to an unheated air jet. As a result, the helium/air mixture jets simulate a heated jet by having a density and velocity more comparable to an actual heated jet. Because the helium/air mixture jets are only a simulation of hot air jets, it is important that the simulation replicate the most important aspects of actual heated jets. The two most distinguishing differences between heated and unheated jets are the lower density and the higher velocity of the hot jets compared to the unheated jets. Stability analyses performed in Refs. 5, 12, 13, and others show that the jet-to-ambient density and acoustic velocity ratios are the dominant factors in determining the stability characteristics and, hence, the noise generation of high-speed jets in this velocity range.

A helium jet exhausting into an air environment can have the same density ratio as an actual hot jet. For example, a perfectly expanded helium (or helium/air mixture) jet would simulate a hot air jet of the same density ratio as follows:

$$(T_j/T_a)_{\text{simulated}} = (\rho_a/\rho_j)_{\text{helium jet}} = (\rho_a/\rho_j)_{\text{hot air jet}} \qquad (1)$$

For shock containing jets operating off design, these relations would need to be modified to account for the unequal static pressure between the jet and the ambient environment.

Whereas this shows that helium/air mixture jets can be used to simulate the density ratio of an actual hot jet, it is important that the jet velocity of the hot jet be simulated as well. Because helium has a higher acoustic speed than air, a helium/air mixture jet operating at the same Mach number as a pure air jet will also have a higher jet velocity. This can be seen by comparing the jet exit velocities of an air jet and a helium/air mixture jet at the same Mach number.

Table 1 shows several important jet and gas properties for two helium/air mixture jets (cases B and C) and for two relevant heated Mach 1.5 jets (cases D and E), all with the same exit velocity. The helium concentration is calculated by mass, not molar, quantities. Properties of an unheated Mach 1.5 jet (case A) are also listed for comparison. Cases A, B, and D are for jets exhausting into standard atmospheric temperature conditions resulting in an ambient acoustic speed of 343 m/s. Cases C and E are for jets exhausting into an environment other than standard day air conditions. Case E will be shown shortly to be the hot jet conditions most comparable to the simulation reported in this work. The temperature and density ratios listed in Table 1 are actual values calculated from isentropic relations. The specific heat ratios for the jets are also listed.

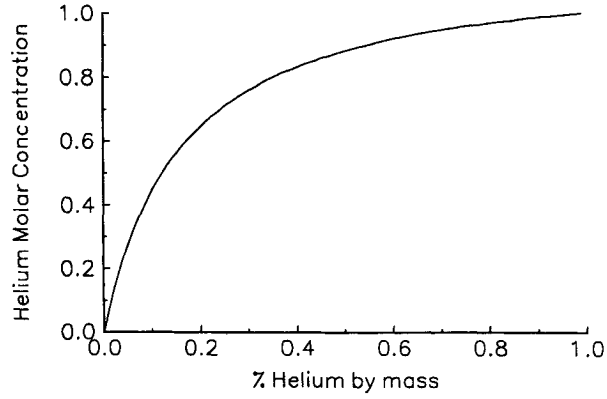

Fig. 1 Helium molar content as a function of helium mass concentration.

Because both the gas constant R and the ratio of specific heats γ vary with helium concentration, it is not possible to exactly match the jet exit velocity and density to the heated pure air jet exhausting into standard day conditions. Note in Table 1 that, whereas the jet exit velocity is matched by the helium/air jet (case B), the jet density is not equivalent to the actual hot jet case exhausting into a similar environment (case D). However, a match of the appropriate nondimensional ratios can be achieved if the ambient air is allowed to absorb some helium, thus raising its effective temperature and lowering its density accordingly. Cases C and E in Table 1 show this match. Therefore, to match the jet-to-ambient density and velocity ratios of an actual heated jet, some helium is allowed to remain in the sealed anechoic chamber of the jet noise facility during testing.

Jet Mixture Concentration

If the gas properties of the mixture (such as the specific heat ratio and the gas constant) are known, standard isentropic relationships can be used to determine the jet Mach number, velocity, temperature, and density. For a binary gas mixture such as the one in this work, it is straightforward to calculate these quantities as long as either the mass fraction or mole fraction of each constituent is known. Figure 1 shows the molar concentration of helium in a helium/air mixture as the mass fraction of helium is increased. Because of the low molecular weight of helium compared to air, the molar content of the jet mixture increases rapidly as the mass fraction of helium is increased, and small amounts of helium in the mixture can have a relatively large effect on the thermodynamic characteristics of the mixture. A complete description of the methodology used to determine the thermodynamic characteristics of a binary gas mixture can be found in most fundamental thermodynamic books and is also described by Kinzie[10] for this particular application.

Because it is possible to determine the gas mixture properties if either the helium or air concentration of the mixture is known, it is necessary to develop a procedure to mix the upstream helium and air supplies such that the mixture molar content is known and can be controlled. Figure 2 shows a schematic of the upstream supply lines and important points in the system. The key to determining the mixture concentration is to ensure that the airflow and the helium flow each pass through a choked valve before mixing. The mass flow through a choked orifice is constant regardless of changes to the flow

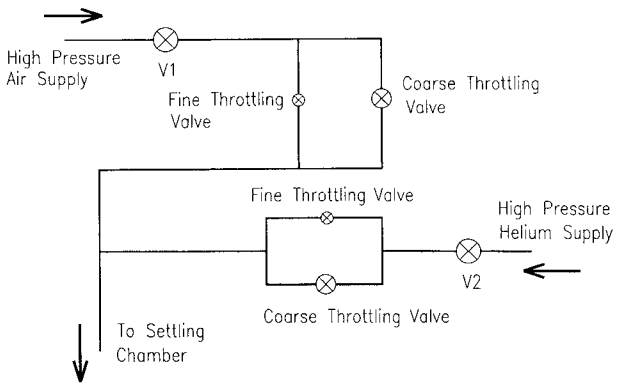

Fig. 2 Schematic of upstream supply lines and critical choke points needed to set the helium concentration of the jet flow.

conditions downstream of the choke point, and this guarantees that the mass flow of each gas into the system will not change once conditions upstream of the choke points are set. These choke points are shown as V1 and V2 in Fig. 2. The pressure upstream of these points is maintained at approximately 2.5 atm while the pressure downstream of these points is typically less than 0.5 atm, thereby ensuring that these valves are choked for any operating condition within the scope of this work.

The mass flow through a choked orifice can be described by

$$\frac{\dot{m}\sqrt{T_0}}{A^* P_0} = \sqrt{\frac{\gamma}{R}\left(\frac{2}{\gamma+1}\right)^{(\gamma+1)/(\gamma-1)}} \tag{2}$$

Therefore, the mass flow through the orifice is dependent only on the orifice size, the total temperature and total pressure upstream of the orifice, and the gas composition. The right-hand side of Eq. (2) will be a constant for any given specific heat ratio and gas constant, which for the present work will be a unique function of helium concentration of the gas mixture. This constant is referred to as Fliegner's constant F. For air ($\gamma = 1.4$, $R = 287$ kJ/kg · K) and helium ($\gamma = 1.67$, $R = 2077$ kJ/kg · K) Fliegner's constants are $F_{\text{air}} = 0.0404$ and $F_{\text{he}} = 0.0159$, respectively.

Because the nozzle throat is also a choke point and because the supply valves V1 and V2 remain choked when the flows are combined, the mass flow of the mixture will be

$$\dot{m}_{\text{mix}} = \dot{m}_{\text{air}} + \dot{m}_{\text{he}} = \frac{P_{0,\text{mix}} A_t}{\sqrt{T_0}} \cdot F_{\text{mix}}(\gamma, R) \tag{3}$$

where $F_{\text{mix}}(\gamma, R)$ is Fliegner's constant for the mixture. Fliegner's constant for the mixture, F_{mix}, is a function only of the mixture specific heat ratio and gas constant.

The procedure to determine the helium concentration in the jet mixture is to set the upstream supply valves that control $P_{0,\text{air}}$ and $P_{0,\text{he}}$ and to record each of these mass flows individually in the absence of flow from the other gas. Then $P_{0,\text{mix}}$ is recorded when the gases are combined. Once Fliegner's constant F_{mix} is known from Eq. (3) and the individual mass flow rates, the concentration of helium in the mixture can be found by determining what mass fraction of helium is required to satisfy Eq. (2). When the helium concentration of the mixture is known, the gas properties of the flow can be calculated.

Helium Concentration in Test Chamber

In the present facility, the ambient gas density changes as helium builds up in the chamber during an experiment. As seen from Table 1, this change in density allows both the jet-to-ambient acoustic velocity ratio and density ratio of the simulation to match those of an actual hot jet. However, hot jets are only simulated if there is a large difference in gas properties between the jet flow and ambient environment. To reduce the effect of the helium buildup, laboratory air is bled into the chamber during an experiment to dilute the helium that is present.

The helium concentration in the chamber is determined from a method that measures the speed of sound in the chamber surrounding

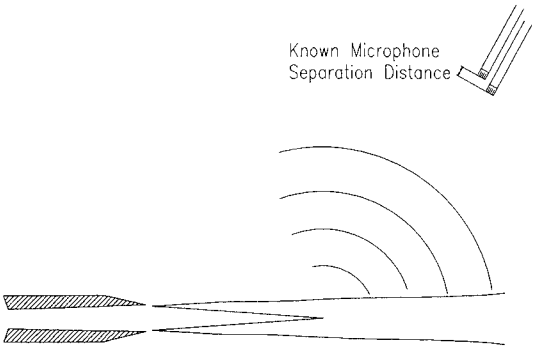

Fig. 3 Schematic showing dual microphone setup used to measure ambient sound speed and helium concentration.

the jet. This is done by using two phase-matched microphones with a known separation distance and by measuring the phase difference of various spectral components of the radiated noise, as shown in Fig. 3. By separating the microphones by a known distance and pointing them at the approximate sound source location in the jet (typically near the end of the jet potential core), the phase difference between the microphone signals allows the speed of sound in the chamber to be calculated. It is also known that the sound speed in the chamber can be calculated from

$$a_{\text{ch}} = \sqrt{R_{\text{ch}} \gamma_{\text{ch}} T_{\text{ch}}} \tag{4}$$

In this expression, a_{ch} is measured from the dual microphone phase difference, and T_{ch} is measured from a thermocouple in the test chamber. Because both R_{ch} and γ_{ch} are related uniquely to the amount of helium in the chamber, the helium concentration in the ambient environment can be found by determining what concentration of helium results in values of R_{ch} and γ_{ch} that give the measured sound speed. McLaughlin et al.[9] give a detailed description of this procedure.

Small amounts of helium in the chamber typically result in an ambient helium concentration on the order of about 7% by mass. In terms of the simulation, the increase in ambient sound speed due to the helium corresponds to a simulated ambient temperature higher than the standard value of 293 K. As earlier discussed, this results in a lower simulated temperature ratio than if the jet were exhausting into pure air, but also a temperature ratio that produces the desired jet-to-ambient acoustic velocity and density ratios.

A test of the helium delivery system was made by shutting off the outside bleed supply and operating a given helium/air jet until the chamber environment had approximately equalized with the jet mixture concentration. The dual microphone system in this case measures a helium concentration in the chamber equivalent to the jet helium concentration set using the flow control valves. The test showed that the two methods agreed within 1% over a wide range of helium/air mixture concentrations. Because each of these methods is independent of one another, the good agreement between the calculated and measured helium concentrations serves as a check on the accuracy of both methods. The results of the helium concentration calibration are also a check on the premise that the strong induced convective stirring of the test chamber by the jet ensures that spacial variations in helium concentrations are minimal. The reader is referred to Ref. 10 for more details on this calibration.

Experimental Facility

A schematic of the jet noise anechoic chamber is shown in Fig. 4. Its dimensions are $0.7 \times 0.8 \times 1.1$ m, and it is lined with acoustic foam 5 cm thick, which produces an effectively anechoic environment for frequencies above 1 kHz. Ambient pressures of around $\frac{1}{15}$ of an atmosphere are established into which the small supersonic jets are exhausted. For these experiments, the exit pressure of the jet flow is maintained within 2% of the ambient chamber pressure to produce relatively shock-free perfectly expanded jets. A recent description of the operation of this facility at Pennsylvania State University can be found in Refs. 8–11.

Both an elliptic and round nozzle were tested. The elliptic nozzle used for this research has an aspect ratio of 3:1 and is designed for

shock-free flow with a nominal exit Mach number of 1.5. The nozzle exit has a major axis length of 24 mm and a minor axis length of 8 mm. The exit area of the nozzle is 151 mm^2, which is equivalent to an axisymmetric nozzle with diameter $D_{eq} = 13.8$ mm. The equivalent diameter D_{eq} is used as the length scale for nondimensionalizing the experimental results. The round nozzle is also designed to be shock free at a Mach number of 1.5 and has a diameter of 10 mm and exit area of 78.5 mm^2. The elliptic nozzle is fitted with one glow discharge electrode located in each quadrant. Because the electrodes are located just outside the nozzle exit, very close to the flow, the modulating local high temperature perturbs the jet shear layer at the chosen frequency with minimal disturbance to the jet flow. By phasing the electrodes separately, different azimuthal modes can be excited in the jet. Kinzie and McLaughlin[8] give a detailed description of the glow discharge technique.

Table 2 shows the experimental conditions (within 2%) reported in this paper for the near perfectly expanded pure air jets and the simulated hot jets. The conditions are the same as in case C of the helium/air jets listed in Table 1 and simulate a hot jet most closely represented by case E. Although both the circular and elliptic jet nozzles were designed to operate at the nominal Mach number 1.5, the circular nozzle ran at $M = 1.6$ for the present experiments. This is because this nozzle was originally designed to operate in the lower Reynolds number range ($Re < 1 \times 10^4$) with boundary-layer corrections included in the nozzle contour design. Operation at higher Reynolds number produces a thinner boundary layer with more nozzle expansion to the higher Mach number. When operating the helium/air mixture jets, the helium concentration is set such that both jets have the same exit velocity, within experimental uncertainty. Throughout this paper, the temperature ratio for all air jets will be nominally referred to as $T_j/T_a = 0.69$, and all helium/air mixture jet cases will be referred to nominally as $T_j/T_a^* = 1.2$. In addition, the 0% helium concentration cases will be referred to as pure air jets, whereas the helium/air mixture jets are referred to as helium/air jets or simply helium jets.

Table 2 Experimental conditions, $Re = 2.7 \times 10^4$

Nozzle shape	M_j	D_{eq}, mm	Jet He concentration (by mass), %	ρ_a/ρ_j (T_j/T_a^*)	u_j, m/s	P_0, torr	P_j, torr	f_c, Hz
Elliptic	1.5	13.8	0	0.69	425	101	28	30,800
Circular	1.6	10	0	0.66	445	160	37	44,500
Elliptic	1.5	13.8	26	1.2	690	185	47	50,000
Circular	1.6	10	23	1.1	690	240	51	69,000

Results and Discussion

The results shown are intended to highlight the difference between the pure air jets and the helium/air mixture jets and to show the effectiveness of the heated jet simulation. Where possible, comparisons are made of the results from the helium simulation with actual hot jet experiments or simulations. Only limited analysis and interpretation of the results are provided here, and more detail can be found in Refs. 8, 10, and 11.

The centerline velocity distributions of the pure air elliptic jet are compared to those of the helium/air mixture jet ($T_j/T_a^* = 1.2$) in Fig. 5. The velocity distribution of the helium jet shows an increased decay rate compared to the air jet with a very slight decrease in potential core length. According to the work of Lau[3] on axisymmetric jets, the potential core region generally contracts as the jet is heated, accompanied by a corresponding faster decay of the centerline velocity. For a Mach number of 1.4, Lau shows a decrease in potential core length from approximately 6 to 4.5 diameters as the jet temperature is increased from isothermal to $T_j/T_a = 2.32$. Because the elliptic jet already has a shorter potential core than the circular jet[11] and the simulated temperature ratio in the present work is not large, the present data appear to agree with the trends observed from the work of Lau[3] in actual heated jets.

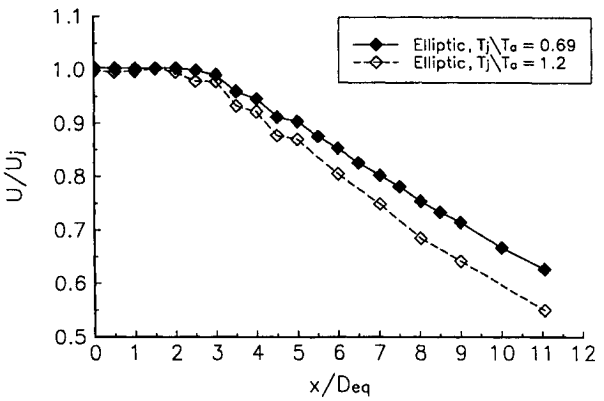

Fig. 5 Centerline velocity distributions for pure air and helium/air mixture jets.

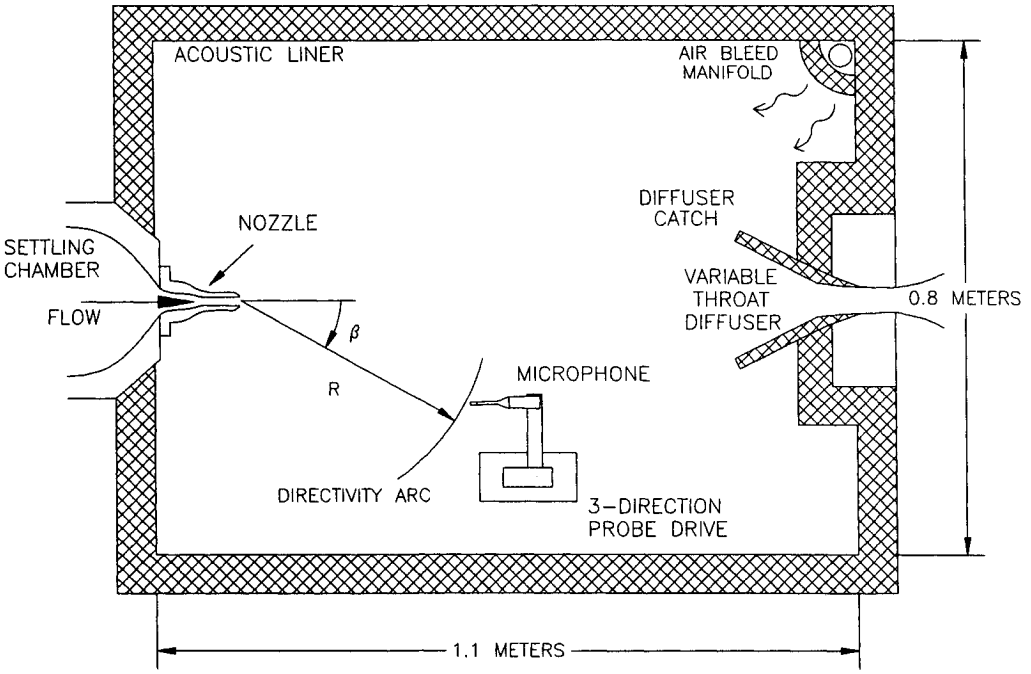

Fig. 4 Facility anechoic chamber.

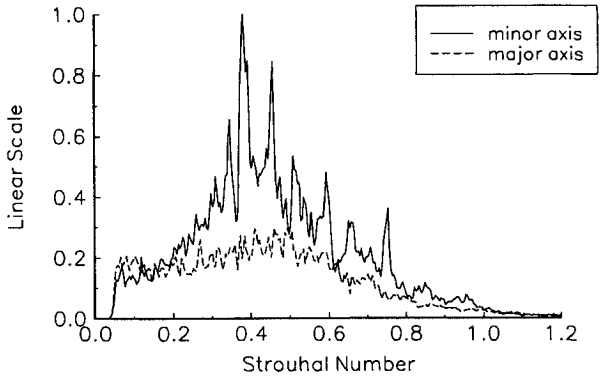

Fig. 6 Hot-wire spectra: $x/D_{eq} = 3.0$, elliptic jet, $T_j/T_a = 0.69$.

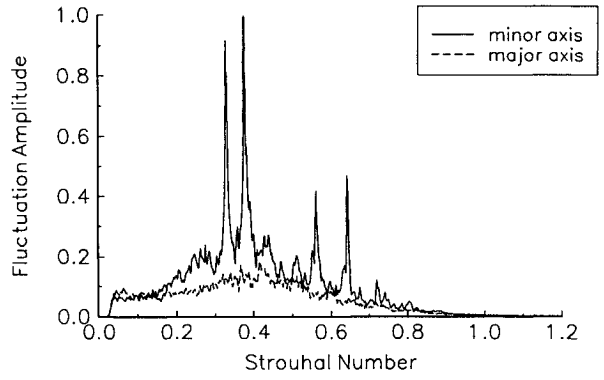

Fig. 7 Hot-wire spectra: elliptic jet, $x/D_{eq} = 3.0$, $T_j/T_a^* = 1.2$.

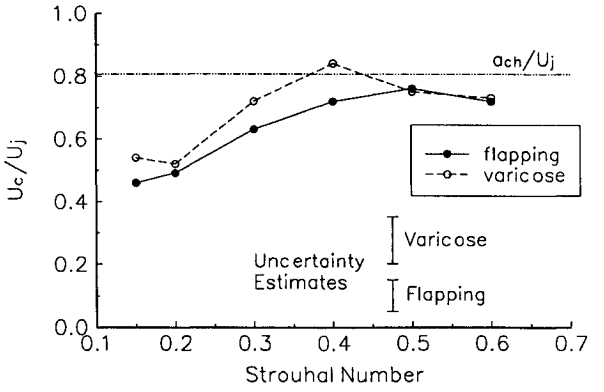

Fig. 8 Phase speed as a function of Strouhal number in artificially excited pure air elliptic jet (downstream of potential core): $T_j/T_a = 0.69$.

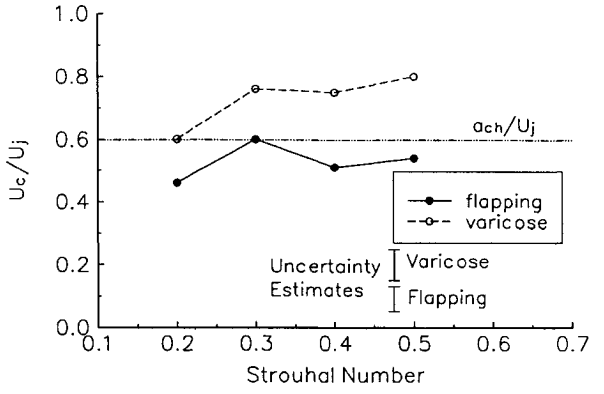

Fig. 9 Phase speed as a function of Strouhal number in artificially excited helium/air elliptic jet (downstream of potential core): $T_j/T_a^* = 1.2$.

Figures 6 and 7 show measured hot-wire spectra at the location of maximum fluctuation level in the jet for both the air and the helium conditions. The amplitudes are normalized by the maximum value in the minor axis plane of each jet. The highest energy levels are centered close to a Strouhal number of 0.4 for both cases. Note, however, that the characteristic frequency of the helium jet is higher than the corresponding air jet (see Table 2). These general spectra occur for both cases at a downstream distance of $x/D_{eq} = 3.0$, close to the end of the potential core. This dominant frequency of $Sr = 0.4$ is predicted by the stability analysis of Morris and Bhat[12] to be the most highly amplified component for a Mach 1.5, $AR = 3$, elliptic jet. In terms of frequency content and relative energy levels, the spectra for the air jet and the helium jet look very similar. It is also clear from these data that the minor axis plane fluctuations contain more energy than those of the major axis plane. This is true for all axial locations throughout the potential core region.

As mentioned earlier, an important property of the instability waves in regard to sound generation is the phase velocity of the instability waves with respect to the ambient environment. Supersonic traveling waves will radiate sound to the far field directly as Mach waves. As reported by Kinzie and McLaughlin,[11] the phase velocity of the instability waves can be measured by cross correlating the glow excitation signal with a hot-wire signal located at various downstream locations in the jet shear layer.

Figure 8 shows the phase velocity of the instability waves as a function of Strouhal number for the pure air elliptic jet. In general, the varicose mode has a higher velocity than the flapping mode, and the phase velocity increases with increasing Strouhal number, except at higher frequencies. The horizontal line represents the phase velocity that is equivalent to the ambient speed of sound normalized by the jet exit velocity. Therefore, phase velocities above this value may radiate noise through Mach wave emission. Except for the varicose mode at $Sr = 0.4$, no Strouhal number component exceeds this value for the air jet case.

Figure 9 shows the same measurements for the helium/air elliptic jet. Again, the varicose mode shows a higher velocity compared to the flapping mode. The stability analysis of Morris and Bhat[12] also predicts the varicose mode to have a higher phase velocity than the flapping mode for both the cold and heated jet conditions. They also predict the phase velocity of both modes relative to the jet exit velocity to decrease as the jet is heated. In general, the present measurements also show these trends. Therefore, these results agree with the predictions of Morris and Bhat that jet heating causes the instability wave phase velocity to increase with respect to the ambient sound speed but to decrease with respect the jet exit velocity.

Note that for the helium case, the phase speed of the varicose mode exceeds the ambient speed of sound over nearly the entire Strouhal number range, whereas the flapping mode is close to, but just below, the sonic value. Tam and Morris[13] showed that near sonic instability waves can have supersonic wave number components that will radiate to the far field. Evidence of the stronger coupling of the hydrodynamic pressure field to the acoustic field at the higher jet velocity is seen in the modal decomposition measurements of the helium elliptic jet reported by Kinzie and McLaughlin.[8] They showed a significant increase of the flapping mode in the jet acoustic field when helium was added to the jet. Far-field acoustic data to be presented later show evidence that this increase in instability wave phase velocity compared to the ambient sound speed corresponds to an increase in acoustic radiation consistent with Mach wave emission.

Sound pressure level (SPL) directivity arcs from the pure air elliptic and circular jets are shown in Fig. 10. The peak noise levels are between 25 and 30 deg. The minor axis plane of the elliptic jet is louder than the major axis plane. This most likely results from the higher fluctuation levels in the minor axis plane compared to the major axis plane and the higher growth rate of the flapping mode as shown by Kinzie and McLaughlin.[11] The elliptic jet also emits less total noise than the round jet.

Figure 11 shows the same measurements for the helium jets. The peak noise angles for the helium jet cases have increased to between 30 and 35 deg. The major axis plane of the elliptic jet is 4–5 dB quieter than the circular jet. Also, the relative difference between the major and minor axis planes of the elliptic jet has increased making the major axis plane of the elliptic jet even quieter compared

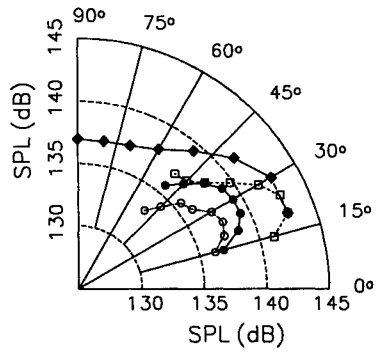

Fig. 10 SPL directivity arcs: R/D_{eq} = 25, T_j/T_a = 0.69; ●, elliptic minor axis; ○, elliptic major axis; □, circular jet; and ♦, M*S prediction for circular jet.

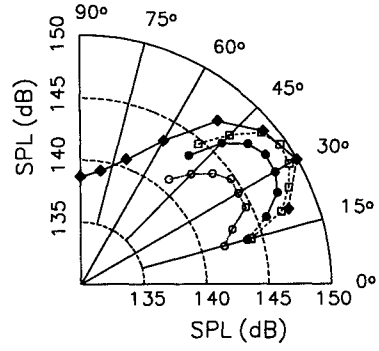

Fig. 11 SPL directivity arcs: R/D_{eq} = 25, T_j/T_a^* = 1.2; ●, elliptic minor axis; ○, elliptic major axis; □, circular jet; and ♦, M*S prediction for circular jet.

to the minor axis plane. A similar phenomenon was also observed by Seiner et al.[4] in measurements of a heated Mach 1.5 elliptic jet. These changes as the jet velocity is increased are attributed to stronger contributions from Mach wave emission to the radiated sound field in the helium/air mixture jet. The increased relative noise suppression at higher velocities is attributed to the ability of the noncircular jet to mix faster compared to the axisymmetric jet. As a result, Mach wave emission, which becomes more powerful as the jet velocity increases, is suppressed more by the increased mixing characteristics of the noncircular jet at the higher jet velocity compared to the lower velocity conditions.

Whereas the helium simulation clearly reproduces many qualitative characteristics of actual hot jets, it is also important to show that the simulation is able to reproduce quantitative changes in SPL and directivity. Because actual hot data were not available for these conditions, noise predictions for the circular jet were made using the M*S noise prediction methodology described in Ref. 14. The predictions are included with the measured data in Figs. 10 and 11. M*S is a well-established semi-empirical prediction tool used in industry for the prediction of noise radiated from high-speed heated jets. M*S was developed using correlation data from a number of actual hot jet experiments. To better compare the trends of the present experimental data with the predictions, the peak SPL value for the predictions of the unheated jet was matched to the peak SPL value of the pure air experimental jet, and that difference was added to all of the predicted values. Therefore, a constant value of 3.3 dB was added to the M*S predictions for both the unheated and heated jet cases. With this minor adjustment to the predictions, the comparison between the measured and predicted directivities are quite good. In particular, the quantitative changes in overall SPL and directivity as the simulated jet temperature increases agree well with the actual hot jet prediction. This comparison is evidence of the ability to accurately simulate the noise generation characteristics of actual heated jets using the helium/air simulation.

Far-field acoustic spectra at the location of peak noise emission are shown in Fig. 12 for the pure air elliptic jet case. The energy peaks around a Strouhal number of 0.25 with the major and minor axis planes showing approximately equal energy in the lower frequency range. The higher SPL levels measured in the minor axis plane come from spectral contributions above a Strouhal number of 0.4.

Figure 13 shows the acoustic spectra at the location of peak noise emission for the helium elliptic jet. As seen in the SPL measurements, the absolute energy levels from the helium/air jets are much

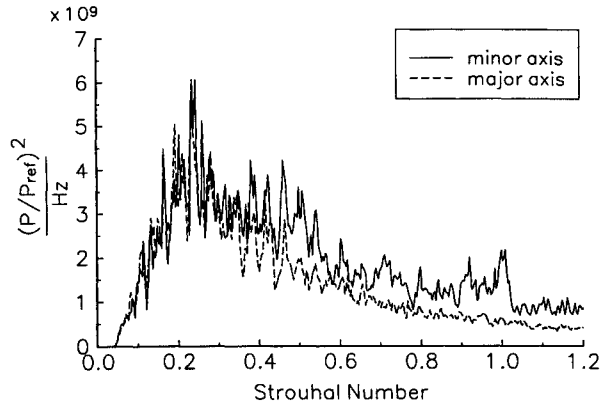

Fig. 12 Acoustic spectra: elliptic jet, R/D_{eq} = 25, β = 25 deg, T_j/T_a = 0.69.

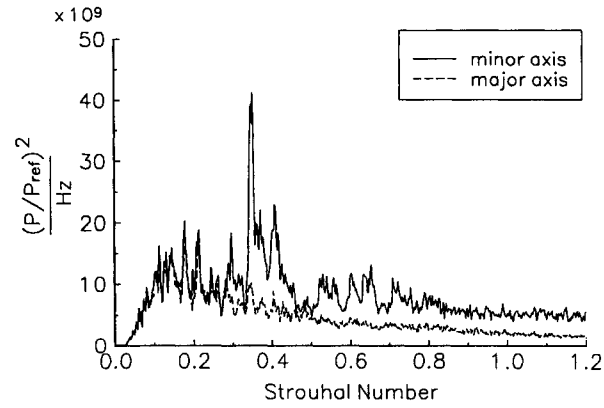

Fig. 13 Acoustic spectra: elliptic jet, R/D_{eq} = 25, β = 30 deg, T_j/T_a^* = 1.2.

higher than from the pure air jet. Again, as with the pure air jets, the lower frequencies have approximately equal amplitude on the major and minor axis planes. However, at Strouhal numbers above 0.3, the minor axis plane of the helium/air jet shows significantly more energy than the major axis plane.

Note that the peak acoustic frequencies for the air case tend to be lower than the peak fluid dynamic fluctuations measured by the hot wires (see Fig. 6) indicating a nonlinear relationship between the flow fluctuations and the radiated noise. For the helium simulation, however, the acoustic spectrum on the minor axis plane is very similar to that measured by the hot wire in the jet shear layer (Fig. 7). Kinzie and McLaughlin[8] used a near-field modal decomposition technique to show that, for the helium/air case, these increased Strouhal number components above $Sr = 0.3$ are composed primarily of the jet flapping mode. Because of the increased phase velocity of the flapping mode relative to the ambient environment, it is believed that these Strouhal number components now radiate directly to the far field. It is clear from these data that the noise generation process from the simulated hot jet is quite different from the cold jet and that these differences are consistent with similar measurements from actual heated jets.

Conclusions

These results show that the helium simulation is able to capture the important noise and flowfield characteristics of an actual heated jet. These data also demonstrate that there are significant differences between cold and heated asymmetric jets with regard to how the fluid dynamics of the jets produce noise. Many of these observations have already been made for the case of heated round jets. Most of the measurement trends agree favorably with the elliptic jet stability analysis of Morris and Bhat,[12] and the measured changes in overall SPL and directivity of the circular jet were in good agreement with the semi-empirical prediction methodology of Ref. 14.

Higher hot-wire fluctuation levels were measured in the minor axis plane than in the major axis plane. Measurements show that,

for the simulated heated jet, the instability waves obtain a phase speed close to or higher than the ambient sound speed, producing a capability for the jet to radiate noise through the Mach wave emission process. The varicose mode always has a higher phase speed than the flapping mode. However, because the flapping mode has a higher growth rate and higher overall fluctuation levels in comparison to the varicose mode, the flapping mode contributes more strongly to the far-field noise.

Acoustic measurements show that the simulated hot jets radiate more noise to the far field at a higher angle to the jet axis compared to the air jet case. Higher SPLs were measured in the minor axis plane than in the major axis plane. These increased levels are attributed to the higher flow fluctuations in the minor axis plane, the faster growth of the flapping mode, and the stronger coupling of the hydrodynamic pressure field to the radiated acoustics as the jet flapping instability achieves a higher phase velocity. For the helium/air case, noise levels in the major axis plane of the elliptic jet were 4–5 dB lower than for the axisymmetric jet. Also for the helium/air case, far-field acoustic spectra were found to contain spectral content similar to the near-field hot-wire spectra. The far-field acoustic spectra of the air jet had a lower frequency content than the hot-wire spectra. These aerodynamic and acoustic observations are consistent with the theory of Mach wave radiation.

These experimental results show that the helium/air simulation captures the dominant characteristics of actual heated jets. In addition, this approach facilitates the use of diagnostic techniques such as hot-wire anemometry and glow discharge active control, which are difficult, if not impossible, in conventional hot jet laboratory experiments. Even though the simulation requires some compromise of the actual physics of a hot jet, the additional insight gained by the use of these diagnostic techniques makes the helium/air simulation a valuable resource in the study of high-speed jet noise.

Acknowledgments

This research project has been supported by NASA Langley Research Center through Grant NAG-1-1047, monitored by J. M. Seiner. The authors are also grateful to P. J. Morris for helpful discussions about this work.

References

[1]Morrison, G. L., and McLaughlin, D. K., "Noise Generation by Instabilities in Low Reynolds Number Supersonic Jets," *Journal of Sound and Vibration*, Vol. 65, No. 2, 1979, pp. 177–191.

[2]Tanna, H. K., Dean, P. D., and Fisher, M. J., "The Influence of Temperature on Shock-Free Supersonic Jet Noise," *Journal of Sound and Vibration*, Vol. 39, No. 4, 1975, pp. 429–460.

[3]Lau, J., "Effects of Exit Mach Number of Temperature on Mean-Flow and Turbulence Characteristics in Round Jets," *Journal of Fluid Mechanics*, Vol. 105, 1981, pp. 193–218.

[4]Seiner, J. M., Ponton, M. K., Jansen, B. J., and Lagen, N. T., "The Effects of Temperature on Supersonic Jet Noise Emission," German Society for Aeronautics and Astronautics (DGLR)/AIAA Paper 92-02-046, 1992.

[5]Tam, C. K. W., and Chen, P., "Turbulent Mixing Noise from Supersonic Jets," *AIAA Journal*, Vol. 32, No. 9, 1994, pp. 1774–1780.

[6]McLaughlin, D. K., Morrison, G. L., and Troutt, T. R., "Experiments on the Instability Waves in a Supersonic Jet and Their Acoustic Radiation," *Journal of Fluid Mechanics*, Vol. 69, Pt. 1, 1975, pp. 73–95.

[7]Troutt, T. R., and McLaughlin, D. K., "Experiments on the Flow and Acoustic Properties of a Moderate Reynolds Number Supersonic Jet," *Journal of Fluid Mechanics*, Vol. 116, 1982, pp. 123–156.

[8]Kinzie, K. W., and McLaughlin, D. K., "Azimuthal Mode Measurements of Elliptic Jets," *Physics of Fluids*, Vol. 9, No. 7, 1997, pp. 2000–2008.

[9]McLaughlin, D. K., Barron, W. D., and Vaddempudi, A. R., "Acoustic Properties of Supersonic Helium/Air Jets at Low Reynolds Number," German Society for Aeronautics and Astronautics (DGLR)/AIAA Paper 92-02-047, 1992.

[10]Kinzie, K. W., "Aeroacoustic Properties of Moderate Reynolds Number Elliptic and Rectangular Supersonic Jets," Ph.D. Dissertation, Dept. of Aerospace Engineering, Pennsylvania State Univ., University Park, PA, Aug. 1995.

[11]Kinzie, K. W., and McLaughlin, D. K., "Noise Radiated from Asymmetric Supersonic Jets," Confederation of European Aerospace Societies (CEAS)/AIAA Paper 95-014, 1995.

[12]Morris, P. J., and Bhat, T. R. S., "The Spatial Stability of Compressible Elliptic Jets," *Physics of Fluids*, Vol. 1, No. 1, 1995, pp. 185–194.

[13]Tam, C. K. W., and Morris, P. J., "The Radiation of Sound by the Instability Waves of a Compressible Plane Turbulent Shear Layer," *Journal of Fluid Mechanics*, Vol. 98, Pt. 2, 1980, pp. 349–381.

[14]Gliebe, P. R., Motsinger, R. E., and Sieckman, A., "High Velocity Jet Noise Source Location and Reduction, Task 6 Supplement—Computer Programs: Engineering Correlation (M*S) Jet Noise Prediction Method and Unified Aeroacoustics Prediction Model (M*G*B) for Nozzles of Arbitrary Shape," Federal Aviation Administration, RD-76-79, Vol. 6a, Sept. 1978.

M. Samimy
Associate Editor